

## Effects of Current Collectors on Electrochemical Performance of FeS<sub>2</sub> for Li-ion Battery

Yourong Wang<sup>\*</sup>, Hantao Liao, Jia Wang, Xiaofang qian, Yuchan Zhu, Siqing Cheng

Chemical and Environmental Engineering Department, Wuhan Polytechnic University, Wuhan 430023, Hubei, P.R.China

<sup>\*</sup>E-mail: [wyrong@whpu.edu.cn](mailto:wyrong@whpu.edu.cn)

*Received:* 1 February 2013 / *Accepted:* 22 February 2013 / *Published:* 1 March 2013

---

The effects of current collectors on the electrochemical performance of FeS<sub>2</sub> electrode have been investigated by applying three types of current collectors, including an Al foil, a Cu foil and a Ni foil. The results show that Ni current collector can greatly improve the discharge capacity and cycle ability of FeS<sub>2</sub> electrode compared to the Al current collector. Cyclic voltammetry and electrochemical impedance spectroscopy also show that the electrodes on the Ni foil show much smaller polarization and lower impedance. Although Cu foil is utilized as anode current collector in the conventional lithium ion batteries, it can react with FeS<sub>2</sub> during the charge/discharge process, so Cu current collector may also be unsuitable to other metallic sulfide electrode except CuS electrode for lithium ion batteries. These results mean that adopting Ni foil as the current collector is more suitable for metallic sulfide electrodes.

---

**Keywords:** Current collector; Electrochemical properties; Lithium ion battery; FeS<sub>2</sub> electrode; Cyclic voltammetry

### 1. INTRODUCTION

In recent years, there has been increasing interest in FeS<sub>2</sub> electrode material for lithium ion batteries because of its high theoretical capacity (890 mAh g<sup>-1</sup>), low cost and non-toxicity [1-3]. However, there are still some obstacles for FeS<sub>2</sub> from being applied as electrode materials for LIBs. One of the serious problems of the Li/ FeS<sub>2</sub> batteries is a rapid drop in capacity during cycling at room temperature [4-8]. In order to solve the problem, several approaches have been performed for improving the cycle performance such as Fe addition [9], coating carbon on the surface of FeS<sub>2</sub> [10] or modifying the liquid electrolytes by adding 1, 3-dioxolane [11]. Throughout the research of lithium ion batteries, the major stream of the FeS<sub>2</sub> battery research has focused on the modification ‘inside’ of the

cathode and electrolyte. But recent investigation shows that current collector is also playing an extremely important role in the rechargeable lithium ion battery [12]. Its physical and chemical properties can impact the performance of lithium ion batteries. Different current collectors can result in significant difference on the performances of the lithium ion batteries. Lee et al. [13] demonstrated that cycle-life of the silicon–graphite composite electrode had significantly been improved by using a Cu current collector with a modified surface morphology. Wang et al. [14] reported that a porous silicon–carbon anode on a carbon fiber current collector had superior overall capacity, cycle ability, and rate capacity.

On the basis of the fact that current collectors impact the performance of lithium ion batteries, we study in this work the effects of three different types of current collectors on the electrochemical performance of FeS<sub>2</sub> positive electrode, including an Al foil, a Ni foil and a Cu foil. Cyclic voltammetry and electrochemical impedance were measured to understand the mechanism of different electrochemical performance.

## 2. EXPERIMENTAL

All reagents were analytically pure from the commercial market and were used as received without further purification. Polyethylene glycol (PEG, the average molecular weight: 200). The sample FeS<sub>2</sub> was prepared in the following procedure: 0.20 g PVP were dissolved in the mixed solution of 10ml distilled water and 10ml polyethylene glycol, then 1 mmol of ferrous sulfate septihydrate (FeSO<sub>4</sub>·7H<sub>2</sub>O) was added to this solution under constant stirring to form a homogeneous solution. 5 mL of sodium hydroxide (0.75 M) was added dropwise into the solution, and finally 0.20 g of sulfur powder (S) was added to the solution under magnetic stirring for 30 min. Then the mixture was sealed in a Teflon-lined stainless steel autoclave, and heated at 180 ° C for 12 h. After reaction, a black powder was obtained by centrifugation, washed with ethanol and water several times, and then dried in oven at 80° C.

The composite electrodes were prepared using the following procedure: 0.03g of polyvinylidene difluoride (PVDF) was first added to *N*-Methyl pyrrolidone (NMP) to form the homogenous solution. Then, the prepared powders and acetylene black (the weight ratio of the prepared powders /acetylene black/ PVDF was 7:2:1) were added to the solution above. The obtained mixture was dispersed by utilizing ultrasonic technology. Subsequently, the mixture was dropped to different current collectors (1.0 cm ×1.0cm).

The composite electrodes were subsequently assembled into Coin-type 2016 cells using Metallic lithium as the anode with a micro-porous membrane separator (Celguard<sup>R</sup> 2325,American) and liquid electrolyte mixtures containing 1 mol L<sup>-1</sup> LiClO<sub>4</sub> and a solvent mixture of dimethoxy ethane/ 1,3-dioxolane (2:1, v/v).The cells were assembled in a glove box filled with pure argon.

The electrochemical properties of the composite electrodes were measured by a program-controlled Battery Test System (Land<sup>®</sup>, Wuhan, China). The charge and discharge characteristics of the composite electrodes were evaluated in the voltage range of 1.0–2.5 V vs. Li<sup>+</sup>/Li<sup>0</sup> at room temperature. Cyclic voltammetry (CV) was performed at potential scan rate of 0.1 mV s<sup>-1</sup> in a three-

electrode cell with lithium foil as counter and reference electrodes by using a CHI 660B Electrochemical Work-station (Chenghua, Shanghai, China). In EIS measurement, the excitation voltage applied to the cells was 10 mV and the frequency range was 100 kHz to 0.1 Hz

### 3. RESULTS AND DISCUSSION

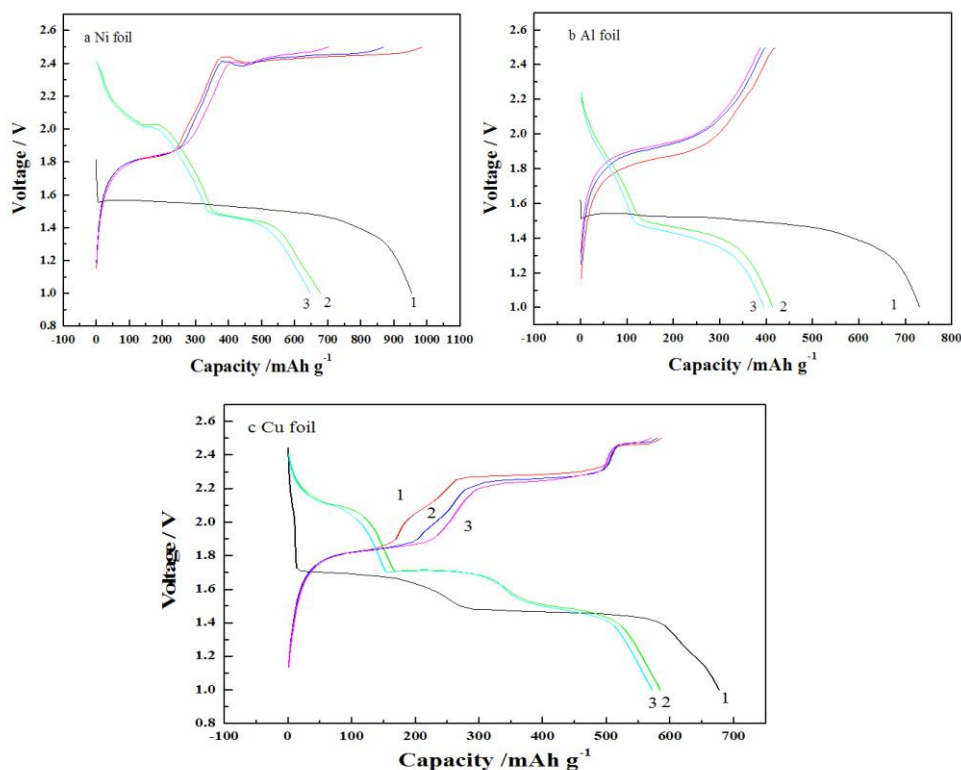


**Figure 1.** Discharge–charge curves of  $\text{FeS}_2$  electrodes on different current collectors between 1.0 and 2.5 V at  $445 \text{ mA g}^{-1}$ . a Ni foil; b Al foil; c Cu foil.

The charge–discharge curves of  $\text{FeS}_2$  positive electrodes on different current collectors are shown in Fig. 1. From Fig. 1(a) and (b), it can be seen that both of the first discharge curves show an abrupt drop in voltage, followed with a single plateau about 1.5 V. This is consistent with the previous reports that the  $\text{FeS}_2$  electrode showed one-voltage-step reduction at ambient temperature, which led to the direct formation of  $\text{Li}_2\text{S}$  and Fe [15-16].

In the subsequent discharge process, a second plateau at ca. 2.0 V is observed, which differs from the first one. The detailed mechanisms for oxidation and reduction of lithium and  $\text{FeS}_2$  during discharge–charge were already reported [17]. Compared to the electrode on the Al foil, the electrode on the Ni foil shows a longer discharge voltage plateau and smaller polarization, and it delivers a higher initial discharge capacity of  $955.1 \text{ mAh g}^{-1}$ . Relatively rapid capacity degradation from the first to the second cycle for both  $\text{FeS}_2$  electrodes is seen, which is attributed to the surface oxidation of the active materials [18, 19]. Nonetheless, the electrodes on the Ni foil still deliver higher

capacities which are  $678.8 \text{ mAh g}^{-1}$ ,  $648.9 \text{ mAh g}^{-1}$  in the second and third cycles, which is a better value reported for this material [3, 10]. From the result above, it can be concluded that the  $\text{FeS}_2$  electrodes on the Ni foil have the better electrochemical performance than those on the Al foil. The differences of the electrochemical performance on the different metal foil will be discussed later.

Fig. 1c shows the charge–discharge curves of  $\text{FeS}_2$  positive electrode on the Cu foil. It is noteworthy that there are significantly different in discharge–charge curves. There are two discharge voltage plateaus observed in the first cycle, which are about at 1.65 V and 1.5 V. Moreover, the third discharge voltage plateau is observed in the subsequent cycles. Accordingly there are three charge voltage plateaus observed. The results indicate that the  $\text{FeS}_2$  electrode maybe make a chemical reaction with the Cu foil. It can be deduced that  $\text{CuS}$  is formed on the  $\text{FeS}_2$  electrode on the basis of the characteristics of the charge-discharge curves, which is reported in our previous study [20]. So the charge-discharge curves on the Cu foil are not analogous to those of the  $\text{FeS}_2$  cells. The mixture can deliver the better capacities which reach  $585.5 \text{ mAh g}^{-1}$  and  $572.8 \text{ mAh g}^{-1}$  in the second and third cycles.

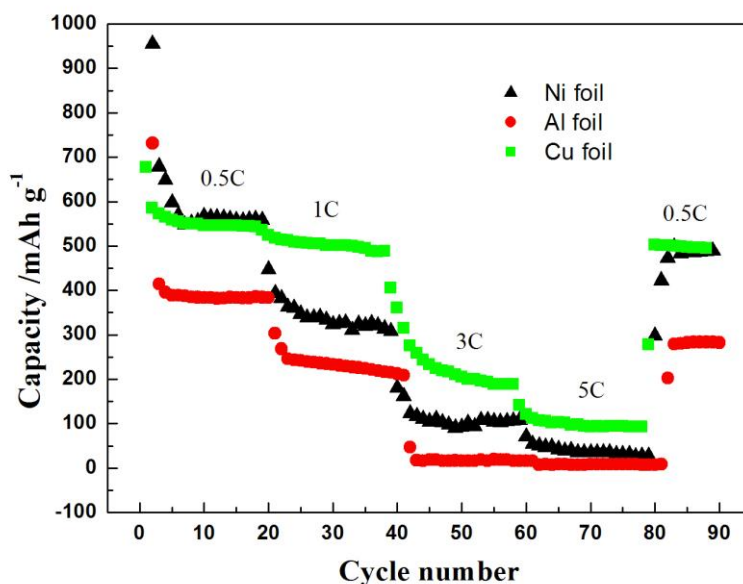


**Figure 2.** The cycle performances of  $\text{FeS}_2$  electrodes at various current densities between 1.0 and 2.5 V,  $\blacktriangle$  Ni foil  $\bullet$  Al foil  $\blacksquare$  Cu foil

Fig. 2 shows the cycle performances of  $\text{Li}/\text{FeS}_2$  cells tested at various current densities. As shown, the  $\text{FeS}_2$  electrodes on the Al foil show the lowest capacities at all the adopted current rates. At 0.5 C rates, the  $\text{FeS}_2$  electrodes on the Cu foil exhibit nearly the same capacities as those on the Ni foil, but the electrodes on the Cu foil show remarkable capacity improvement at higher current rates. This result may be attributed to the formation of  $\text{CuS}$  on the Cu foil. Our previous studies demonstrate that  $\text{CuS}$  electrodes have a good rate performance. Overall, the current collectors have a great effect on the electrochemical performance of the electrodes, especially under high C-rates. It is also worth noting that after cycling 90 cycles the discharge capacities of the electrodes on the Ni foil and Cu foil still

reach about  $490 \text{ mAh g}^{-1}$ . But the capacity of the electrode on the Al foil is only  $283 \text{ mAh g}^{-1}$ . These results demonstrate that the current collectors have a great effect on the cycling stability nature of the active materials.

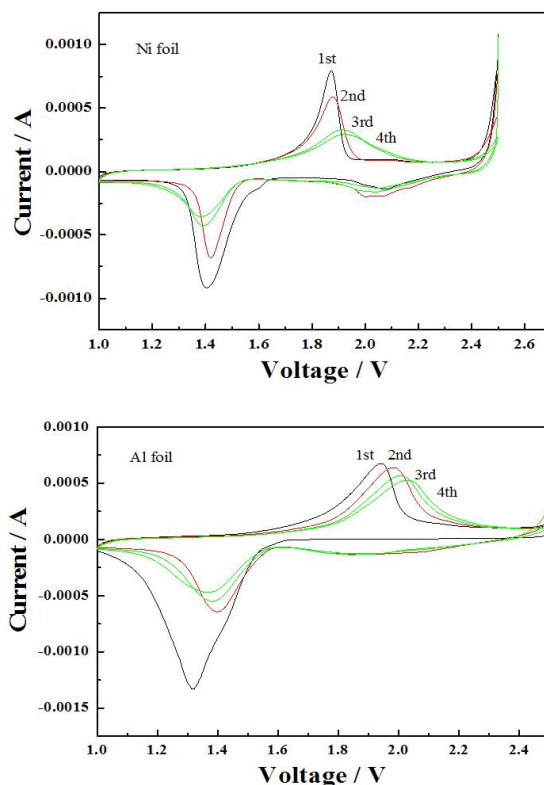


**Figure 3.** Cyclic voltammograms of  $\text{FeS}_2$  electrodes on the Ni foil and Al foil at room temperature. The potential sweep rate is  $0.1 \text{ mV s}^{-1}$  and the voltage range is between 2.5 V and 1.1 V

To understand the electrochemical process and this difference in behavior, CV curves of all the  $\text{FeS}_2$  electrodes between 1.0 V and 2.5 V are recorded in Fig. 3. The shapes of the CV curves are similar for the electrodes on the Ni and Al foil, indicating the same electrochemical behavior of the two electrodes. In the cathodic scan of the first cycle,  $\text{FeS}_2$  follows a two-step lithiation:  $\text{FeS}_2 + 2\text{Li}^+ + 2\text{e}^- \rightarrow \text{Li}_2\text{FeS}_2$  (2 V) and  $\text{Li}_2\text{FeS}_2 + 2\text{Li} + 2\text{e}^- \rightarrow \text{Fe} + 2\text{Li}_2\text{S}$  (1.4 V). In the anodic scans, the material is converted to  $\text{Li}_2\text{FeS}_2$  at around 1.8 V and then to  $\text{Li}_{2-x}\text{FeS}_2$  ( $0 < x < 0.8$ ) at around 2.5 V [21]. At room temperature if the material is driven to high potentials (above 2.5 V), instead of regenerating the  $\text{FeS}_2$ ,  $\text{FeS}_x$  and elemental sulfur may be formed, so the cutoff voltage is set at 2.5 V. Subsequent cycling occurs between  $\text{Li}_{2-x}\text{FeS}_2$  and  $\text{Fe}/\text{Li}_2\text{S}$ .

There is a slight change in the position of the peaks and the redox current reduce slightly with cycling initially; however, they change very little after the first few cycles. Fig. 3 demonstrates that the  $\text{FeS}_2$  electrodes have good cycle stability at room temperature after a few initial cycles, which is consistent with the results presented in Fig 2.

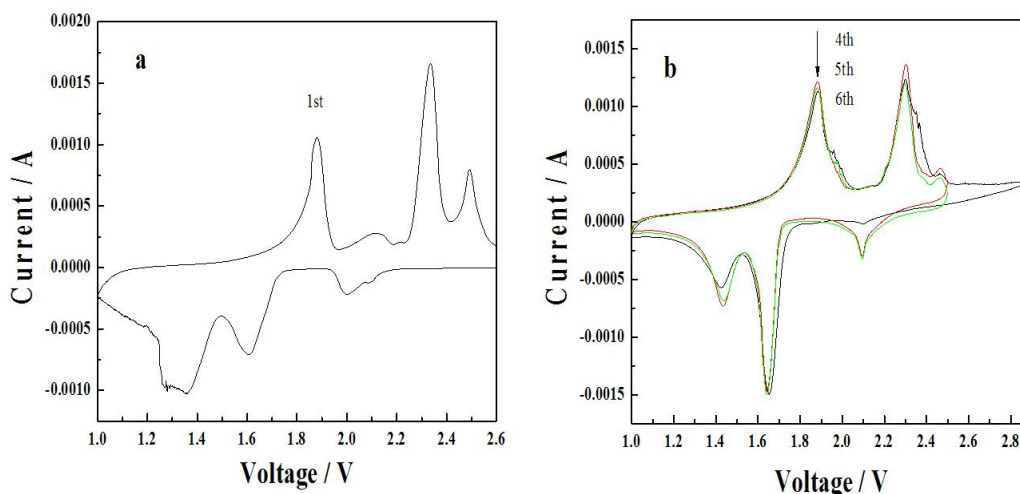


**Figure 4.** Cyclic voltammograms of FeS<sub>2</sub> electrodes on the Cu foil. The potential sweep rate is 0.1 mV

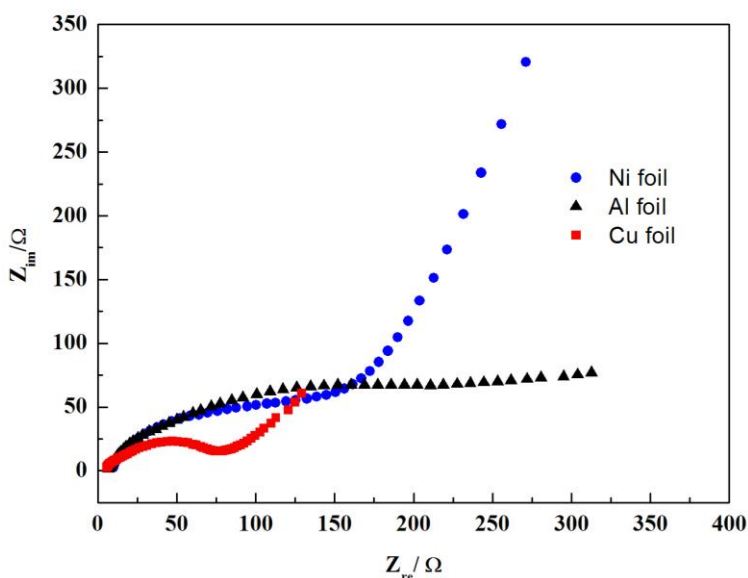


**Figure 5.** Nyquist plots for cells using different current collectors

Compared to the electrodes on the Al foil, the electrodes on the Ni foil deliver the smaller interval between the oxidation and reduction peaks, suggesting the smaller polarization. As is well known, the transferring delay of electrons and lithium ions on the active material/electrolyte interface can result in the polarization in lithium ion batteries [22]. Therefore, the CV curves demonstrate that the electrons and lithium ions can transfer more actively on the Ni foil.

In order to explore the changes of the electrodes on the Cu foil, the CV curves are shown in Fig. 4. From Fig. 4, it can be seen that two additional oxidation/reduction peaks appear at 2.3 V and 1.6 V respectively. This indicates the change in lithium/FeS<sub>2</sub> reactions, which is different to the FeS<sub>2</sub> electrodes on the other two current collectors. The CV curves demonstrate that there are other

chemical reactions on the FeS<sub>2</sub> electrodes using the Cu foil as current collector. Our previous study indicates that CuS is formed during cycling.

The difference in electrochemical behavior of the FeS<sub>2</sub> electrodes on the different metal current collectors is explained by EIS analysis. Fig. 5 shows Nyquist plots of the different FeS<sub>2</sub> electrode from 0.1 Hz to 100 kHz in a three-electrode cell with lithium foil as counter and reference electrodes. It is generally believed that the width of these semi-circles is the sum of the charge-transfer and FeS<sub>2</sub>/metal current collector interfacial resistances [23]. From Fig. 5, it can be seen that the width of these semi-circles on the Cu foil is the smallest, since all the electrodes studied here have the same active material and electrolyte, we expect the same electrochemical behaviors at the solid/electrolyte interface. Therefore, the observed differences in the charge-transfer resistance are apparently associated with the properties of the current collectors. Accordingly, it can be concluded that the interfacial resistance follows the order of Al > Ni > Cu. EIS analysis indicates that the improved electrochemical performances can be attributed to the lower impedance.

#### 4. CONCLUSION

The electrochemical performance of the FeS<sub>2</sub> electrodes on different current collector has been investigated. It is found that current collector can greatly impact the performance of lithium ion batteries. For the electrode with Cu foil, CuS is formed during cycling, and thereby it is not FeS<sub>2</sub> electrode in the end. The electrodes on the Ni foil display a higher discharge capacity and cycling performance than those on the Al foil. The improved electrochemical performances can be attributed to the smaller polarization and lower impedance. The results in the paper are not limited to the FeS<sub>2</sub> electrodes, can be extended to other metallic sulfide electrodes.

#### ACKNOWLEDGEMENTS

This work is supported by Education Science Foundation of Hubei Province (No. Q20091806), Project of Chinese Ministry of Education (No. 208088) and the National Natural Science Foundation of China (No. 31101370).

#### References

1. S.Y. Huang, X.Y. Liu, Q.Y. Li, J. Chen, *J. Alloys and Compounds*, 472 (2009) L9.
2. D. Zhang, X. L. Wang, Y. J. Mai, X. H. Xia, C. D. Gu, J. P. Tu, *J. Appl. Electrochem.*, 42 (2012) 263.
3. T. Takeuchi, H. Kageyama, K. Nakanishi, Y. Inada, M. Katayama T. Ohta, H. Senoh, H. Sakaebe, T. Sakai, U. Tatsumi, H. Kobayashi, *J. Electrochem. Soc.*, 159 (2) (2012) A75.
4. E. Peled, D. Golodnitsky, E. Strauss, J. Lang, Y. Lavi, *Electrochim. Acta*, 43 (1998) 1593.
5. D. Golodnitsky, E. Peled, *Electrochim. Acta*, 45 (1999) 335.
6. K. Takada, Y. Kitami, T. Inada, A. Kajiyama, M. Kouguchi, S. Kondo, M. Watanabe, M. Tabuchi, *J. Electrochem. Soc.*, 148 (2001) A1085.
7. G. Ardel, D. Golodnitsky, K. Freedman, E. Peled, G. B. Appetecchi, P. Romagnoli, B. Scrosati, *J. Power Sources*, 110 (2002) 152.

8. L. A. Montoro, J. M. Rosolen, J. H. Shin, S. Passerini, *Electrochim. Acta*, 49 (2004) 3419.
9. Y.-J. Choi, W.G. Kang, H.S. Ryu, T.-H. Nam, H.J. Ahn, K.K. Cho, K.W. Kim, K.S. Ryu, *Mater. Technol.*, 27 (1) (2012) 124.
10. B. Wu, H.H. Song, J.H. Zhou, X.H. Chen, *Chem. Commun.*, 47 (2011) 8653.
11. E. Strauss, D. Golodnitsky, E. Peled, *Electrochem. Solid State Letter*, 2 (1999) 115.
12. Q.N. Sa, Y. Wang, *J. Power Sources*, 208 (2012) 46.
13. Y.L. Kim, Y.K. Sun, S.M. Lee, *Electrochim. Acta*, 53 (2008) 4500.
14. U. Guo, A. Sun, C.S. Wang, *Electrochem. Commun.*, 12 (2010) 981.
15. L. A. Montoro, J. M. Rosolen, *Solid State Ionics*, 159 (2003) 233.
16. J.W. Choi, G. Cheruvally, H.J. Ahn, K.W. Kim, J.H. Ahn, *J. Power Sources*, 163 (2006) 158.
17. Y. Shao-Horn, Y.S. Osmialowski, Q.C. Horn, *J. Electrochem. Soc.*, 149 (2002) A1547.
18. Ph. de Donato, C. Mustin, R. Benoit, R. Erre, *Appl. Surf. Sci.*, 68 (1993) 81.
19. E. M. Shembel, Y. V. Polischuk, O. V. Chervakov, D. Reisner, *Ionics*, 12 (2006) 41.
20. Y.R. Wang, X.W. Zhang, P. Chen, H.T. Liao, S.Q. Cheng, *Electrochim. Acta*, 80 (2012) 264.
21. Z.C. Yang, J.G. Shen, N. Jayaprakash, Lynden A. Archer, *Energy and Environmental Science*, 5(5) (2012) 7025.
22. D. Zhang, J.P. Tu, J.Y. Xiang, Y.Q. Qiao, X.H. Xia, X.L. Wang, C.D. Gu, *Electrochim. Acta*, 56 (2011) 9980.
23. H.C. Wu, Eric Lee, N.L. Wu, T. Richard Jow, *J. Power Sources*, 197 (2012) 301.